this work is that, based on the triplet-state rotational relaxation times and k_m results for 4-PP, the rotational relaxation times of the triplet state for this phosphor are directly related to the temperature-dependent portion of k_m in the approximate temperature range 193-93 K.

ACKNOWLEDGMENT

The methanol and water solvents donated by Burdick & Jackson, and the samples of β-cyclodextrin donated by American Maize-Products Company are greatly appreciated.

Registry No. β-CD, 7585-39-9; 4-PP, 92-69-3; NaCl, 7647-14-5.

LITERATURE CITED

(1) Hurtubise, R. J. *Solid Surface Luminescence Analysis*; Dekker: New York, 1981.
(2) Hurtubise, R. J. *Phosphorimetry: Theory, Instrumentation and Applications*; VCH: New York, 1990; Chapters 6-8.
(3) Bello, J. M.; Hurtubise, R. J. *Appl. Spectrosc.* **1986**, *40*, 790-794.
(4) Richmond, M. D.; Hurtubise, R. J. *Anal. Chem.* **1989**, *61*, 2643-2647.
(5) Bello, J. M.; Hurtubise, R. J. *Appl. Spectrosc.* **1988**, *42*, 619-624.
(6) Bello, J. M.; Hurtubise, R. J. *Anal. Chem.* **1988**, *60*, 1291-1296.
(7) Richmond, M. D.; Hurtubise, R. J. *Anal. Chem.* **1991**, *60*, 169-173.
(8) Ramasamy, S. M.; Hurtubise, R. J. *Appl. Spectrosc.* **1989**, *43*, 616-621.
(9) Ramasamy, S. M.; Hurtubise, R. J. *Anal. Chem.* **1987**, *59*, 432-436.
(10) Ramasamy, S. M.; Senthilnathan, V. P.; Hurtubise, R. J. *Anal. Chem.* **1986**, *58*, 612-616.
(11) Ramasamy, S. M.; Hurtubise, R. J. *Talanta* **1989**, *36*, 315-320.
(12) Turro, N. J. *Modern Molecular Photochemistry*; Benjamin/Cummings: Menlo Park, CA, 1978.
(13) Morrison, L. E.; Weber, G. *Biophys. J.* **1987**, *52*, 367-379.
(14) Rutherford, H.; Soutar, I. *J. Polym. Sci.: Polym. Phys. Ed.* **1977**, *15*, 2213-2225.
(15) Rutherford, H.; Soutar, I. *J. Polym. Sci.: Polym. Lett. Ed.* **1978**, *16*, 131-136.
(16) Rutherford, H.; Soutar, I. *J. Polym. Sci.: Polym. Phys. Ed.* **1980**, *18*, 1021-1034.
(17) Dalterio, R. A.; Hurtubise, R. J. *Anal. Chem.* **1983**, *55*, 1084-1089.
(18) Guillet, J. *Polymer Photophysics and Photochemistry*; Cambridge University Press: Cambridge, MA, 1985.
(19) Zlatekvich, L., Ed. *Luminescence Techniques in Solid State Polymer Research*; Dekker: New York, 1989.

RECEIVED for review December 11, 1990. Accepted March 7, 1991. Financial support for this project was provided by the Department of Energy, Office of Basic Energy Sciences, Grant No. DE-FG02-86ER13547.

Structure of Alkylated Silica Surfaces: Quenching of Fluorescence from Covalently Bound Pyrene

A. L. Wong, M. L. Hunnicutt, and J. M. Harris*

Department of Chemistry, University of Utah, Salt Lake City, Utah 84112

The influence of overlying solvent on the structure of alkylated silica surfaces is investigated. In these experiments, [3-(1-pyrenyl)propyl]dimethylchlorosilane (3PPS) was chemically bonded at low coverages to silica gel, which was further modified with monomeric C1, C8, and C18 ligands. Fluorescence lifetimes of 3PPS were measured to determine the differences in the interfacial polarity of these materials in methanol and methanol/water solution. Rates of quenching by mercuric chloride were also measured to correlate differences in polarity with the exposure of the immobilized probe to solvent. For C1-modified and bare silica, the results indicate an interfacial environment that is dominated by exposure to solvent. On C18-modified silica, access by the surface-bound probe to the quencher is minimal, indicating that the long alkyl chains limit exposure of the underlying silica to the solvent. The most interesting behavior was exhibited by C8 ligands, which produce an interfacial environment where the probe has limited contact with the solvent in methanol but becomes much more exposed in 75/25% methanol/water. This change in environment was attributed to the collapse of the alkyl ligands, driven by hydrophobic interactions that reduce their contact with the aqueous solution.

There has been a growing interest in better understanding the surface microenvironment of chemically modified silica materials. These materials not only play a key role in reversed-phase liquid chromatography, but they are also used for solute preconcentration and immobilization of analytical reagents. The structure of ligands immobilized to silica at the liquid/solid interface contributes to the selectivity of chromatographic stationary phases and the behavior of surface-bound reagents. Fluorescence spectroscopy has been found to be a powerful tool for in situ investigations of modified silica/liquid interfaces. Lochmüller and co-workers pioneered this approach by covalently attaching fluorescent probe molecules to silica to determine the polarity (*1*) and microheterogeneity (*2*) of the interface and the organization and distribution of bound ligands (*3*, *4*). Other investigators have measured the fluorescence spectra of physisorbed probes to study the polarity of *n*-alkyl stationary phases (*5*-*8*), the heterogeneity of surface environments (*7*), ion pair interactions (*9*, *10*), and temperature-induced changes in the interface structure (*11*, *12*). Interesting differences can arise between the interface structure and polarity as reported by bound and physisorbed probes or between sorbed probes of differing hydrophobicity (*6*, *8*). Covalently bound molecules are constrained to report conditions at the silica surface, while the physisorbed probes are free to minimize their free energy of sorption in different regions of the interface (*6*, *8*) with varying degrees of alkyl chain reorganization (*8*, *13*).

Time-resolved fluorescence spectroscopy has also been used to characterize the structure and dynamics at alkylated silica surfaces in contact with liquids. Measuring the kinetics of excimer emission from immobilized pyrene probes has allowed solvent-induced changes in the conformations of surface-bound ligands to be investigated (*4*, *14*). Rates of excimer formation by pyrene physisorbed at C18-derivatized surfaces have provided estimates of the microviscosity of the interfacial layer (*15*, *16*). Time-resolved measurements of diffusion-controlled quenching of fluorescence from covalently bound pyrene have

0003-2700/91/0363-1076$02.50/0

recently been employed to estimate the maximum rates of bimolecular reactions at silica/solution interfaces (*17, 18*). In the former study (*17*), the decay of fluorescence from pyrene immobilized on fumed (pyrogenic) silica was not a single-exponential function indicative of a dispersion of surface environments arising most likely from a distribution of surface silanol groups. In the latter study (*18*), differences between the rates of fluorescence quenching at the interface and those in free solution could be quantitatively attributed to the solution volume excluded from the vicinity of the fluorescent probe by the silica surface.

Pyrene is a particularly useful probe for the time-resolved fluorescence studies since interactions with its local environment (surface silanols, solvent, and neighboring ligands) alter the distribution of electron density and the symmetry of the pyrene π-electron system (*19*). These perturbations promote mixing in pyrene between the lowest energy short axis-polarized B_u^2 excited state and the long axis-polarized B_u^1 state at slightly higher energy (*20*). Radiative transitions from this latter state are more strongly allowed, and thus the fluorescence lifetime of pyrene depends upon the degree of state mixing and therefore its local environment (*21*). The electronic interactions are responsible also for the changes in the vibronic band structure in the fluorescence emission spectrum, which has been used extensively for characterizing the polarity of the alkylated silica/solution interface (*5–7, 11, 12*).

In this study, both fluorescence decay times and fluorescence quenching rates of immobilized pyrene are measured in order to study how alkyl chains shield the silica surface from the overlying solvent. Fluorescence lifetimes of the immobilized probes on the different surfaces generally increase as the alkyl chain lengths of the bonded ligands increase. A polar, unretained quencher, mercuric chloride, is added to the methanol solvent to determine the accessibility of the immobilized probe to the solvent on C18, C8, C1, and bare silica surfaces. The results indicate that the bound probe is well protected by the C18-alkyl chains, partially protected from the solvent by shorter C8 chains, and fully exposed to solvent on the C1 and bare silica surfaces. When the solution phase is changed to 75/25% methanol/water, the C8-alkyl chains appear to collapse, increasing the exposure of the pyrene moiety to solution.

EXPERIMENTAL SECTION

Materials. Porous microparticulate silica VYDAC (mean pore diameter of 300 Å, N_2 BET surface area 90 m^2/g, mean partial diameter 10 μm) was used in the preparation of the alkylated silica materials. Preparation and subsequent derivatization of [3-(1-pyrenyl)propyl]dimethylchlorosilane (3PPS) onto silica are described in detail elsewhere (*19*). Chlorosilane reagents, trimethylchlorosilane (Aldrich 98%), *n*-octyldimethylchlorosilane (Petrach), and *n*-octadecyldimethylchlorosilane (Aldrich 98%), were used without further purification in the alkylation of the pyrene-bonded silicas. Reagent-grade anhydrous triethylamine (Fisher 98%) were used as a catalyst. The condensation reaction was carried out in spectrograde chloroform (Omnisolv 99.9%) dried and stored over molecular sieves. Solutions of varying concentrations of mercuric chloride (Fisher ACS certified) in methanol (Omnisolv) and water (purified in-house, Corning glass distilled and fed to a Barnstead, Nanopure system) mixtures were prepared by using standard volumetric techniques.

Alkylation of Pyrene-Bonded Silica. Reactions were carried out under a dry, inert nitrogen atmosphere in a three-neck 100-mL round-bound flask equipped with an addition funnel, condenser, and Teflon stir bar. All glassware had been previously treated with trimethylchlorosilane to deactivate surface silanols and dried at 140 °C. Predried microparticulate silica gel previously modified at low coverage with 3PPS (2.0 g) was transferred to the reaction flask and dried at 140 °C for 12 h prior to chemical treatment. All solvents and reagents were added under dry nitrogen purge via a glass syringe. Anhydrous triethylamine (2 mL, 14.4 mmol) was added to the silica slurry prior to silane addition for base-catalyzed reactions. Reaction mixtures were refluxed for 6 h, with the silica being vigorously dispersed by stirring in 50 mL of chloroform.

Silane mixtures were prepared by transferring silanes into an addition funnel and subsequently diluting with 10 mL of chloroform. A total of 10 M equiv silane per silanol was added at a rate of 5 M equiv silane per silanol per minute into a vigorously stirred slurry. The surface silanol density used in the above calculation was 8 μmol/m^2. The reaction mixture was stirred and refluxed for 6 h after the initial transfer. The silica was then filtered through a glass frit and successively washed with (3 × 100 mL) of chloroform, tetrahydrofuran, acetonitrile, methanol, and acetone. The surface now chemically modified with both the 3PPS probe and alkyl ligands was dried under vacuum at 60 °C/10 mTorr for 12 h and stored in a desiccator prior to analysis.

Analytical Methods. Elemental carbon analyses (MHW Laboratories, P.O. Box 15149, Phoenix, AZ 85018) were obtained to determine the silica surface concentration of alkylsilane. The method of Unger and co-workers (*21*) was used to calculate surface concentrations. By using these methods, the amount of 3PPS reagent bound on the silica surfaces was found to be less than 0.11 μmol/m^2. This coverage corresponds to less than 10% of a monolayer and is sufficiently low to avoid significant probe–probe interactions. At larger surface coverages, interactions between neighboring 3PPS species can be inferred from the observation of excimer emission from excited pyrene which encounters a bound neighbor during its excited-state lifetime (*3, 4*).

To check for excimer emission as a test for the local proximity of bound pyrene groups on the surface, fluorescence emission spectra of the 3PPS probe on the alkylated silicas were recorded. Spectra were collected by using a Farrand optical scanning spectrofluorometer (Model 801) at an excitation wavelength of 305 nm, while the emission monochromator was scanned from 350 to 500 nm. Excimer emission at 470 nm was found to be less than 10% of the peak monomer emission intensity for all of the silicas studied. This result confirms the small fractional surface coverage by the probe and its dispersed bonding over the silica surface.

Chromatographic retention of mercuric chloride was measured on bare and alkylated silica surfaces with methanol and 75/25% methanol/water mobile phases by utilizing the following columns packed with silicas comparable to those used in the spectroscopic studies: porous silica (Analytichem International, 25 cm × 2.51 mm), C1 silica (E.S. Industries), C8 silica (Whatman Partisil 10 CCS/C8, 25 cm × 2.1 mm), and C18 silica (Whatman Partisil 10 ODS-2, 25 cm × 2.1 mm). A flow rate of 1 mL/min was controlled by a Beckman Model 110A chromatographic pump, and optical absorption at a single wavelength (254 nm) was measured by using a Beckman Model 153 to detect the eluent. Retention values of mercuric chloride on the reversed-phase and bare silica columns were determined relative to D_2O (*22*) and pentane (*23*) dead volume markers for the alkyl-modified silica and bare silica surfaces, respectively.

Fluorescence Decay Kinetics. Time-resolved fluorescence decay curves of the immobilized 3PPS on four different alkylated silica surfaces (C18, C8, C1, and bare silica) suspended in methanol/water solution were collected from 1% (by weight) silica slurries. Oxygen was removed from the sample by three freeze–pump–thaw cycles, after which the slurries were allowed to equilibrate at room temperature for 2 h prior to collecting fluorescence transients. Decay curves were obtained by single photon counting with a laser fluorometer described elsewhere (*24*). A time-to-amplitude converter (Ortec Model 577) and a fast analog-to-digital converter attached to the histogramming memory (Lecroy Model 3515) were used in place of the time-to-digital converter described in ref 24. Fluorescence quenching rates were obtained in six quencher solutions containing different amounts of mercuric chloride over a concentration range of 10^{-4}–10^{-3} M. A minimum of five decay transients was collected at each concentration and analyzed to give an average decay rate.

The decay curves were analyzed with a linear least-squares fit to the log of a single-exponential function, $\ln I = \ln (I_0) - t/\tau$, where I_0 is the intensity at $t = 0$ and τ is the decay time; the fit was properly weighted for the shot noise in the data and the logarithmic conversion (*25*). Decay times were obtained by taking

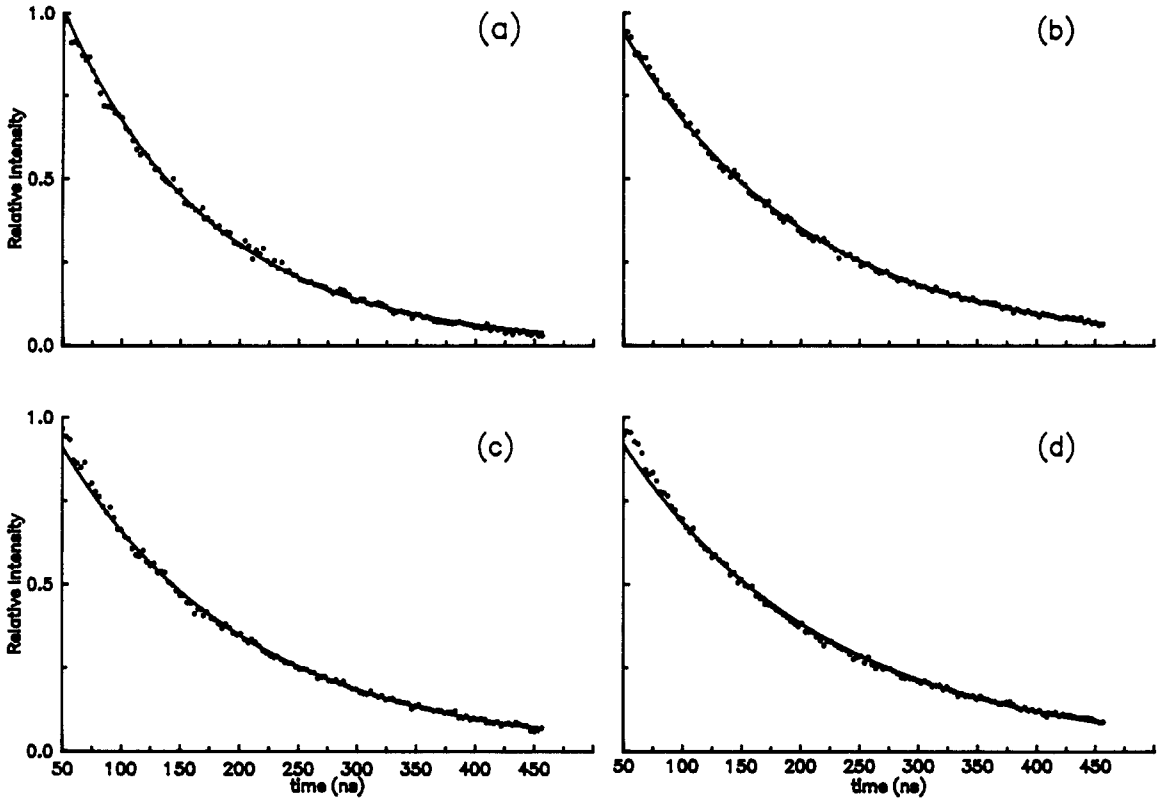

Figure 1. Fit of the last 90% of the pyrene fluorescence decay data to a single-exponential function. Fluorescence emission measured from pyrene immobilized on bare silica (a) and C1 (b), C8 (c), and C18 (d) alkane-modified silica surfaces suspended in methanol. Fluorescence decay signal (points) and single-exponential fit (solid line).

the reciprocal of the least-squares slope when the logarithm of fluorescence intensity was plotted against time. Only the last 90% of the decay curves (50–450 ns) were included in the time-domain analysis due to silica background fluorescence, which decreases rapidly to less than 1% of the pyrene signal within the first 50 ns. Average decay times obtained from five different decay curves are reported.

RESULTS AND DISCUSSION

Fluorescence Lifetime of Bound Pyrene on Silica. The time-resolved fluorescence decay of the covalently bound pyrene probe (3PPS) on bare silica and monomeric C1-, C8-, and C18-alkane-modified silica surfaces suspended in methanol and methanol/water solutions was found to follow first-order single-exponential behavior, as illustrated in Figure 1. Previous studies that utilized the same pyrene probe immobilized on pyrogenic or fumed silica found stretched exponential decay behavior of the form, $I = I_0 \exp[-(kt^{\beta})]$ where $\beta = 0.67$, indicating a distribution of decay rates (*17*). The kinetic inhomogeneity, recovered by Laplace inversion of the decay curves, was attributed to a dispersion of surface energies arising most likely from a distribution of surface silanols on the fumed silica. Since the fluorescence decay of the 3PPS probe on precipitated silica in the present study follows single-exponential decay behavior, a homogeneous environment is indicated for the probe on precipitated or porous silica; any inhomogeneities that might exist on this surface must be sampled and averaged by the probe on the time scale which is shorter than the 150-ns fluorescence decay times.

The measured fluorescence lifetimes of covalently bound pyrene on bare silica and C1-, C8-, and C18-alkylated silica surfaces suspended in methanol systematically increase with increasing alkyl chain length as shown in Table I. The lifetime increases from 164 ns on bare silica to 182 ns on C18-alkylated silica. It is not surprising to observe differences in the lifetime of immobilized pyrene on the different alkylated silica surfaces since the decay kinetics of the fluorophore have been found to be sensitive to local surface environment (*19*, *21*). Interactions with polar surroundings are known to mix the long- and short-axis polarized excited states of pyrene (*20*), which changes the relative intensities of the vibronic bands (*26*) and shortens the fluorescence lifetime (*19*, *27*). Pyrene covalently bound to bare silica exhibits the shortest lifetime, corresponding to the most polar surface environment, while the C18 surface is least polar. Interestingly, the pyrene probe on the C1 surface exhibits a lifetime that is indistinguishable from its behavior on the bare silica surface. This result may indicate that the interface polarity (as measured by interactions with the immobilized pyrene ring) is dominated by the solvent and not the underlying surface. The C8 surface produces an interface polarity that is intermediate between that of bare or C1 silica and the C18 surface. The difference between C8 and C18 environments could be due to variation in solvent intercalation into the alkyl ligands or due to differences in the extent to which the ligands shield the surface bound probe from the overlaying solvent. Since the size of the pyrene ring is comparable to the C8 ligands, difference shielding should play a significant role in the observed interfacial environment. This premise is tested below using fluorescence quenching to measure the accessibility of the fluor to solution.

Table I. Fluorescence Lifetimes of Pyrene (3PPS) Immobilized on Silica

	τ, ns	
surface	100% methanol	75/25% methanol/water
bare silica	163.5 (±0.5)	154.3 (±0.5)
C1 silica	164.2 (±0.5)	153.1 (±0.5)
C8 silica	177.2 (±0.5)	172.0 (±0.5)
C18 silica	182.1 (±0.5)	182.2 (±0.5)

To evaluate the sensitivity of the fluorescent surface probe to changes in solvent composition, a 75/25% (volume/volume) methanol/water solution was substituted for methanol above and fluorescence lifetimes of the 3PPS were measured. The fluorescence lifetime results are summarized in Table I for the bare and derivatized silica surfaces. Comparison of the results from the 3PPS probe indicates a reduction in the lifetime of fluorescence with a more polar solvent on all but the C18-alkylated silica surface. The 3PPS fluorescence lifetimes on bare and silica surfaces continue to reflect an identical response to solution polarity, where their lifetimes are again indistinguishable as they were for the 100% methanol solvent. On the C18 surface, however, no change in the interfacial environment of the silica immobilized probe is observed upon changing the overlying solvent from methanol to 75/25% methanol/water. This result strongly suggests that the C18 ligands fully shield the probe molecules from solution. Furthermore, no change in the degree of methanol intercalation into the C18 layer is indicated since the fluorescence lifetime of the probe remains constant. This is a reasonable conclusion in light of the distribution isotherm results of McCormick and Karger (*22*), who showed that monomeric C18 ligands are fully saturated with methanol when the volume fraction of methanol in water exceeds 30%.

Somewhat different behavior was observed by Carr and Harris (*6*) in the polarity of monomeric C18 surfaces inferred from the fluorescence vibronic band intensities of pyrene *physisorbed* to the C18 surface. Increases in the interfacial polarity reported by this sorbed probe could be observed with solutions above 75% methanol concentration, while the present results indicate that a probe immobilized directly to the silica surface is insensitive to changes in solvent composition. This difference in bound versus sorbed probe behavior suggests a gradient in interfacial structure and properties. In light of the methanol isotherm results, the covalently bound fluorescent probe responds to the average composition of the interfacial layer, which is unchanged above 30% methanol. The response of the physisorbed probe, on the other hand, must reflect changes in solvation of hydrophobic sorbed molecules at a C18/solution interface. Since the interfacial tension of a hydrophobic interface is reduced by increasing the concentration of organic modifier in solution, sorbed hydrophobic molecules should come into greater contact with the overlaying solvent as the concentration of organic modifier is increased. Similar conclusions have been drawn from the solvent-dependent behavior of surfactant-like probes at C18 surfaces (*10*) and from the differences in the interfacial behavior of hydrophobic versus hydrophilic probes at C18 surfaces (*8*).

An intermediate change in the interfacial polarity upon substituting methanol/water solution for methanol was observed for the C8-alkylated silica, where the 3PPS probe exhibited a decrease in fluorescence lifetime from 177 ns in methanol to 172 ns in 75/25% methanol/water. The change in fluorescence lifetime of the probe on the C8 surface is about half the change observed for 3PPS on bare and C1 silica surfaces where the probe is fully exposed to solution. This intermediate change in the interfacial polarity of the C8 upon exposure to methanol/water solution could correspond to a change in the structure of the interface. By addition of water to the overlying solvent, one could expect greater hydrophobic interactions with the C8 ligands, leading to a reduction in the contact between these ligands and the solvent. The resulting aggregated or collapsed state for the surface ligands (*28*) would expose the 3PPS probe to the aqueous solution, based on the observed increase interfacial polarity. A test of this proposal is carried out by using a quencher in the solution phase, as described in the following section.

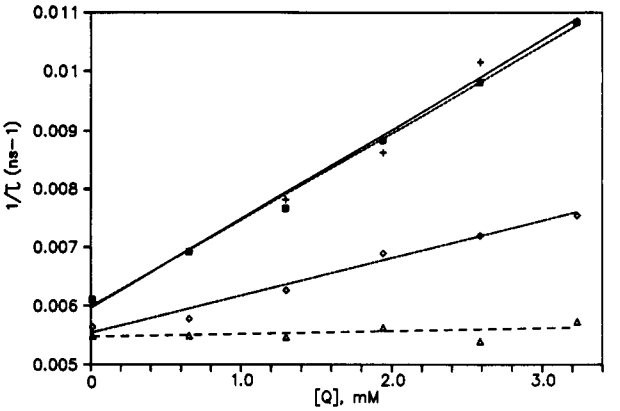

Figure 2. Stern–Volmer plot of the fluorescence decay rates of surface-bound 3PPS ($1/\tau$) versus the concentration of mercuric chloride in methanol. The linear least-squares fits are shown (solid and dashed lines), and the quenching constants (k_q) are obtained from the slopes. Samples are (squares) bare silica, (+) C1 silica, (diamonds) C8 silica, and (triangles) C18 silica.

Quenching Rates of 3PPS on Bare and Alkylated Silica Surfaces. To better understand the solvent-dependent changes in 3PPS fluorescence lifetime and to correlate these differences with the changes in the structure of the interface, rates of quenching by mercuric chloride of the fluorescence from 3PPS immobilized on the bare and alkylated silicas were measured. Mercuric chloride was chosen first for its large quenching efficiency; the rate of quenching the fluorescence from a solution-phase analogue to 3PPS, 1-methylpyrene, by mercuric chloride in methanol was $k_q = 4.8 \times 10^9\ M^{-1}\ s^{-1}$. This quenching rate is indistinguishable from the diffusion-controlled limit, indicating that each collision between mercuric chloride and an excited state of the fluor results in quenching. Thus, differences in the rate of quenching of the surface-immobilized probe by mercuric chloride can be directly related to differences in the rates of encounter between the quencher and probe. Mercuric chloride was also chosen for its large dipole moment (1.43 D in dioxane (*29*)) and negligible affinity for surface silanols, so that its adsorption to alkylated and bare silica is minimal. Chromatographic measurements were carried out to check the affinity of mercuric chloride for bare, C1, C8, and C18 silica surfaces using methanol and 75/25% methanol/water as mobile phases; retention of mercuric chloride was not detectable (minimum detectable capacity factor was $k' \leq 0.08$). The fraction of mercuric chloride that is adsorbed to the silica and modified silica surfaces from solution can, therefore, be neglected. Thus, the measured quenching rates are indicative of encounters between the surface-bound pyrene probe and quencher in solution.

The rate of quenching was measured by obtaining fluorescence decay transients from immobilized pyrene on each of the alkylated silicas suspended in methanol and 75/25% methanol/water solution containing different concentrations of mercuric chloride. The intensity transients continued to follow a single-exponential decay, as above, indicative of a homogeneous population of quenching encounters and diffusion by the quencher in a three-dimensional environment (*18*). The fluorescence decay rates increased linearly with concentration as predicted by a collisional quenching model described by the Stern–Volmer equation

$$1/\tau = 1/\tau_0 + k_q[Q] \qquad (1)$$

where τ_0 is the fluorescence lifetime of 3PPS in the absence of quencher, k_q is the bimolecular quenching rate constant, and [Q] is the concentration of quencher. A plot of the fluorescence decay rate, $1/\tau$, versus the concentration of mercuric chloride in solution for each of the silica surfaces is shown in Figure 2. The quenching rate constants, k_q,

Table II. Rates of Mercuric Chloride Quenching of Fluorescence from 3PPS Immobilized on Silica

surface	$10^{-9}k_q$, M^{-1} s^{-1}	
	100% methanol	75/25% methanol/water
bare silica	1.45 (±0.07)	1.18 (±0.05)
C1 silica	1.50 (±0.10)	1.29 (±0.09)
C8 silica	0.64 (±0.06)	0.93 (±0.1)
C18 silica	0.05 (±0.07)	0.16 (±0.05)

estimated by the slopes of the best fit to a straight line through the data, are summarized in Table II. In methanol, the quenching rates of 3PPS on bare silica and C1-alkylated silica are indistinguishable at 1.5×10^9 M^{-1} s^{-1}. Quenching the pyrene probe immobilized on C8 silica occurs at about half this rate, $k_q = 0.64 \times 10^9$ M^{-1} s^{-1}, while there was no detectable quenching of the bound probe on C18 silica from methanol; that is, k_q is indistinguishable from zero.

Since the fluorescent probe is covalently attached to the silica surface and the quencher is only in the solvent, these quenching rates can be used to infer solvation of the probe and the local structure of the bound ligands in the vicinity of the probe. Since there are no ligands other than the 3PPS probe on the bare silica surface, the fluorescence quenching on this surface establishes a maximum rate of k_q from solution. The quenching of the fluorescence of the probe bound on the C1 surface was indistinguishable from the rate on bare silica. This result is not a surprising result since the pyrene probe, immobilized through a propylsiloxane linkage, extends well away from the surface and is not protected by a C1 ligands. This result supports the conclusion drawn from the unquenched fluorescence lifetimes of the probe that the interface polarity observed by the 3PPS probe on the bare and C1 surfaces is dominated by contact with the solvent.

The fluorescence quenching rate of the immobilized probe on C8 silica is smaller than the maximum rate observed on C1 and bare silica by about 50%, indicating that the probe is only partially accessible to encounters with quencher in solution. Since mercuric chloride does not partition within C8-alkyl chains, the observed quenching rate decrease must arise from partial shielding of the probe from the solvent by the alkyl ligands, reducing the frequency of collisions with solution phase species. The single-exponential decay behavior of the quenched fluorescence further indicates that distinguishable populations of exposed and shielded probes molecules do not exist, at least on the 100-ns time scale of the fluorescence decay of the probe. The longer alkyl chains of the C18 silica surface apparently surround the immobilized 3PPS completely and prevent any collision between the probe and solution-phase species, as indicated by absence of any observable quenching of the fluorescence on the C18 surface. The conclusions regarding the structure of the C8 and C18 surfaces are well supported by the differences in interface polarity inferred from the unquenched fluorescence lifetimes of the probe, discussed above.

The quenching rates of the fluorescence from the bound probes on the bare and alkylated silicas suspended in 75/25% methanol/water solutions can also be rationalized in terms of differences in the structure of the liquid/solid interface. From the data in Figure 3 and the resulting k_q values summarized in Table II, there is again no discernible difference between the rate of mercuric chloride quenching of 3PPS bound to bare and C1 derivatized surfaces. Note that a decrease in the quenching rate in 75/25% methanol/water solution compared to neat methanol is expected due the higher viscosity of the methanol/water solution (*30*). Most interestingly, the rate of fluorescence quenching of pyrene bound on the C8 silica did not decrease in proportion to the C1 and bare silica results but rather increased from 0.64×10^9 M^{-1} s^{-1} in methanol to 0.93×10^9 M^{-1} s^{-1} in 75/25% methanol/water. This latter quenching rate on the C8 surface is only 25% smaller than the rates measured on C1 and bare silica under the same solution conditions. The hydrophobicity of bonded alkyl ligands has been suggested to be a driving force for their collapse in aqueous solutions to minimize contact with the solvent (*28*). Such a collapse of the C8 ligands apparently exposes the pyrene moiety to the solution phase, resulting in nearly complete accessibility to the quencher. The increase in quenching rate correlates with the increase in interfacial polarity (inferred from the 3PPS fluorescence lifetimes above). The reduction in the degree of chain extension of C8 ligands in response to aqueous conditions also produces an interfacial environment for the bound probe which is more polar.

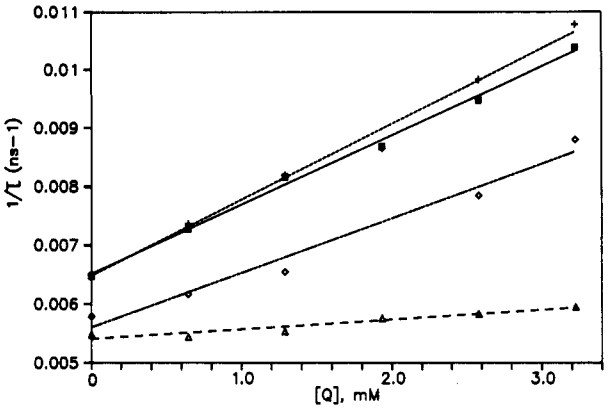

Figure 3. Stern–Volmer plot of the fluorescence decay rates of surface-bound 3PPS ($1/\tau$) versus the concentration of mercuric chloride in 75/25% methanol/water solution. The linear least-squares fits are shown (solid and dashed lines), and the quenching constants (k_q) are obtained from the slopes. Samples are (squares) bare silica, (+) C1 silica, (diamonds) C8 silica, and (triangles) C18 silica.

A small but detectable quenching rate for the 3PPS probe immobilized on C18 silica was observed for the 75/25% methanol/water solvent condition. Despite the minimal change in interfacial polarity as indicated by the unquenched fluorescence lifetime of the probe, the quenching result indicates occasional contact between the probe and a solution-phase quencher. Compared to the undetectable rate of quenching in neat methanol, the finite rate of 3PPS quenching in 75/25% methanol/water solution likely arises from some degree of collapse of the C18 ligands, resulting in partial exposure of the 3PPS probe to the solution. To test for the further changes in the exposure of the C18 silica-bound 3PPS probe to solvents containing higher concentrations of water, a study also was made of the fluorescence lifetime and quenching rates for the C18 silica suspended in 50/50% methanol/water solution. Unlike the results presented thus far, the fluorescence decay transients under these more aqueous conditions are not single-exponential functions. While an appropriate analysis of the kinetics is difficult (*31*), the results clearly indicate some degree of inhomogeneity in the interfacial environment and in the quenching kinetics. Since the 50/50% methanol/water solvent produces measurable retention of mercuric chloride on a C18 surface (*7*), inhomogeneity in quenching kinetics could arise from distinct sorbed versus free solution populations of quencher. The microenvironment polarity of pyrene physisorbed to C18 surfaces has indeed been found to be inhomogeneous under similar conditions, a conclusion drawn from changes in the fluorescence vibronic band intensities versus mercuric chloride concentration (*7*).

Lochmüller and co-workers (*4*, *28*) have suggested that the C18-alkyl chains collapse under aqueous solution conditions to form hydrophobic domains in the form of "islands" or

"clusters". If this model is an accurate representation of the interface, then the exposure of silica-immobilized fluorescent probes to solution should not be homogeneous but dependent upon their distribution within these hydrophobic domains. Some populations may be fully exposed to solution while other populations are minimally exposed. These differences would be reflected in a range or distribution of fluorescence decay times and quenching rates, as long as the domains live longer than the excited states of the probe molecules. Since nonexponential decay behavior is absent in the shorter C8-alkane-modified silica, it is possible that greater mobility of these shorter alkyl chains at room temperature produces an average environment sampled by the pyrene probe during its excited-state lifetime, which appears homogeneous. Further studies to determine the inhomogeneity and structuring of alkyl chains at silica surfaces in more polar solvents are currently in progress.

LITERATURE CITED

(1) Lochmüller, C. H.; Marshall, D. B.; Wilder, D. R. *Anal. Chim. Acta* **1981**, *130*, 31.
(2) Lochmüller, C. H.; Marshall, D. B.; Harris, J. M. *Anal. Chim. Acta* **1981**, *131*, 263.
(3) Lochmüller, C. H.; Colborn, A. S.; Hunnicutt, M. L.; Harris, J. M. *Anal. Chem.* **1983**, *55*, 1344.
(4) Lochmüller, C. H.; Colborn, A. S.; Hunnicutt, M. L.; Harris, J. M. *J. Am. Chem. Soc.* **1984**, *106*, 4077.
(5) Stahlberg, J.; Almgren, M. *Anal. Chem.* **1984**, *57*, 817.
(6) Carr, J. W.; Harris, J. M. *Anal. Chem.* **1986**, *58*, 626.
(7) Carr, J. W.; Harris, J. M. *Anal. Chem.* **1987**, *59*, 2546.
(8) Men, Y.-D.; Marshall, D. B. *Anal. Chem.* **1990**, *62*, 2606.
(9) Dowling, S. D.; Seitz, W. R. *Anal. Chem.* **1985**, *57*, 602.
(10) Shaksher, Z. M.; Seitz, W. R. *Anal. Chem.* **1989**, *61*, 590.
(11) Carr, J. W.; Harris, J. M. *J. Chromatogr.* **1989**, *481*, 135.
(12) Carr, J. W.; Rauchkorst, A. J.; Harris, J. M. Unpublished results.
(13) Dill, K. A. *J. Phys. Chem.* **1987**, *91*, 1980.
(14) Lochmüller, C. H.; Hunnicutt, M. L. *J. Phys. Chem.* **1986**, *90*, 4318.
(15) Bogar, R. G.; Thomas, J. C.; Callis, J. B. *Anal. Chem.* **1984**, *56*, 1080.
(16) Stahlberg, J.; Almgren, M.; Alsins, J. *Anal. Chem.* **1986**, *60*, 2487.
(17) Wong, A. L.; Marshall, D. B.; Harris, J. M. *Can. J. Phys.* **1990**, *68*, 1027.
(18) Wong, A. L.; Hunnicutt, M. L.; Harris, J. M. *J. Phys. Chem.*, in press.
(19) Hunnicutt, M. L.; Harris, J. M.; Lochmüller, C. H. *J. Phys. Chem.* **1985**, *89*, 5246.
(20) Langhlde, F. W.; Thulstrup, E. W.; Michl, J. *J. Chem. Phys.* **1983**, *78*, 3372.
(21) Unger, K. K. *Porous Silica*; Elsevier: New York, 1979.
(22) McCormick, R. M.; Karger, B. L. *Anal. Chem.* **1980**, *52*, 2249.
(23) Synder, L. R. *Principles of Adsorption Chromatography*; Marcel Dekker Inc.: New York, 1968.
(24) Wong, A. L.; Harris, J. M. *Anal. Chem.* **1989**, *61*, 2310.
(25) Bevington, P. R. *Data Reduction and Error Analysis for the Physical Sciences*; McGraw-Hill: New York, 1969.
(26) Dong, D. C.; Winnik, M. W. *Photochem. Photobiol.* **1984**, *35*, 17.
(27) Hunnicutt, M. L.; Wong, A. L.; Harris, J. M. Unpublished studies, University of Utah.
(28) Lochmüller, C. H.; Wilder, D. R. *J. Chromatogr. Sci.* **1979**, *17*, 574.
(29) *Nouveau Traite de Chemie Minerale*; Pascal, P., Ed.; Masson: Paris, 1962; Vol. V.
(30) Bingham, E. C.; White, G. F.; Thomas, A.; Caldwell, J. L. *Z. Phys. Chem.* **1912**, *83*, 41.
(31) Marshall, D. M. *Anal. Chem.* **1989**, *61*, 660.

RECEIVED for review February 7, 1991. Accepted March 8, 1991. This research was funded in part by a grant from the Office of Naval Research. Additional fellowship support (to A.L.W.) from the ACS Division of Analytical Chemistry, and the Society of Analytical Chemists of Pittsburgh is acknowledged.

Simulation of Carbon-13 Nuclear Magnetic Resonance Spectra of Polycyclic Aromatic Compounds

Kyle L. Jensen, Abigail S. Barber, and Gary W. Small*

Department of Chemistry, The University of Iowa, Iowa City, Iowa 52242

Spectra–structure relationships are developed that allow carbon-13 nuclear magnetic resonance chemical shifts to be simulated in a set of diverse polycyclic aromatic compounds. Employing 33 compounds that encompass 24 different aromatic ring backbones, six linear models are generated that allow complete spectra to be simulated to an average error of 0.68 ppm. Successful model generation is found to be dependent upon grouping atoms of similar chemical environments together and the use of structural parameters based on Hückel molecular orbital and molecular mechanics calculations. The computed models are evaluated by use of a separate prediction set of 11 compounds not included in the model generation work. The average spectral prediction error for these compounds is 1.02 ppm, even though seven of the 11 compounds contain ring backbones not found among the 33 compounds used in computing the models.

INTRODUCTION

Spectrum simulation techniques for carbon-13 nuclear magnetic resonance spectroscopy (^{13}C NMR) have potential use in the solution of structure elucidation problems and in the verification of chemical shift assignments. These methods allow the chemical shifts of carbon atoms to be estimated, given only the chemical structure.

The two most widely used approaches to predicting ^{13}C NMR chemical shifts are database retrieval methods (*1*) and empirical modeling techniques (*2–4*). The database techniques are based on the ability to encode the chemical environment of a carbon atom in a form that can be compared to each member of a library of similarly encoded environments and their associated chemical shifts. In a prediction, each estimated chemical shift is taken as the experimentally observed shift associated with the environment in the library that matches most closely to that of the carbon whose predicted chemical shift is desired. The principal drawback to this approach is that the prediction accuracy depends directly on the presence in the library of the appropriate environments. An exact match of the environments must be obtained if an accurate prediction is to be made. In this scheme, there is no capability to use the library data to interpolate the correct chemical shifts.

The modeling techniques attempt to overcome this limi-

0003-2700/91/0363-1081$02.50/0